Laser-Driven Atomic Pump

Petr Král[1] and David Tománek[2]
[1]*Department of Physics, University of Toronto, 60 St. George Street, Ontario, Toronto M5S 1A7, Canada*
[2]*Department of Physics and Astronomy, and Center for Fundamental Materials Research, Michigan State University, East Lansing, Michigan 48824-1116*
(Received 31 August 1998)

We propose a laser-driven pump for atomic transport through carbon nanotubes. A two beam coherent control is used to inject carrier population into the lowest unoccupied nanotube bands, which is *anisotropic* in momentum space. The resulting electron current moves intercalated atoms along the tube. This system is a unique prototype of a single atom deposition machine which overcomes the loading problem of the scanning tunneling microscope. [S0031-9007(99)09502-2]

PACS numbers: 78.20.Jq, 61.48.+c, 66.30.Qa, 85.40.Ux

The demonstrated manipulation and deposition of individual atoms on surfaces with the tip of a scanning tunneling microscope (STM) [1,2] have opened a new era in nanotechnology. The STM enables us to study and modify nanostructures on the atomic scale [3,4] and to explore biomolecules [5]. The limitation of this technique to transport only single atoms prevents us from assembling larger structures. A "continuous STM" would offer a significant improvement here. Similar micromachines, commonly called "molecular motors" [6], can transport ions, atoms and molecules through membranes in biocells or along their tubular cytoskeleton [7].

The recently discovered nanotubes of carbon [8] and other materials [9] are formed with various diameters and chiralities, and their electronic structure varies from semiconducting to metallic [10–12]. The morphology of the hollow tubes provides an excellent possibility to create a nanometer-scale "fountain pen" (pump) with atomic filling. Isolated nanotubes can be filled [13] and nanotube ropes reversibly intercalated [14] during synthesis. The intercalated atoms usually condense into rather immobile aggregates [9,15]. To realize an atomic pump, a new mechanism is needed to move these atoms along the tubes, which could work similar to the mechanism of electron drag by hot carriers [16].

In applied dc electric fields, electromigration [17–19] has been shown to set atoms into motion. Partly ionized atoms are driven by the direct force F_d due to the external field that is locally modified at the atomic site, and by the wind force F_w caused by the reflection of conduction electrons from these atoms. Since F_d usually dominates F_w [18,19], generation of a force to set intercalated atoms into motion would require applying large dc biases, especially for atoms trapped at defects.

More efficient and qualitatively different driving could be realized if the atoms would take better advantage of the large unidirectional momenta and energy carried by the hot electrons. This type of driving can be realized in photovoltaic materials with no inversion symmetry, where a dc current of hot electrons can be generated by light. Only recently, a way has been shown to generate a net electric current by light in semiconductors [20,21], irrespective of their crystal symmetry. Generation of hot carriers with asymmetric population of momenta $\pm\mathbf{k}$, yielding such a current, was induced by quantum interference of one- and two-photon excitations with respective frequencies $2\omega_0$ and ω_0. The direction of the current is *coherently controlled* by the relative phase of the two laser beams. Since no special crystal symmetry is required, a current can be generated in the same way in isolated [22] and bundled [23] single-wall and multiwall carbon nanotubes with different geometrical and electronic structures. This current may displace an added atom in the nanotube, as schematically depicted in Fig. 1, by exerting on it the wind force F_w, due to the absorption of electron momenta. The direct force F_d, caused here by a local charge buildup due to electrons reflected from the atom, is much smaller than F_w.

Here we explore this idea of atomic driving in the $(10, 10)$ carbon nanotube [24]. The model Hamiltonian,

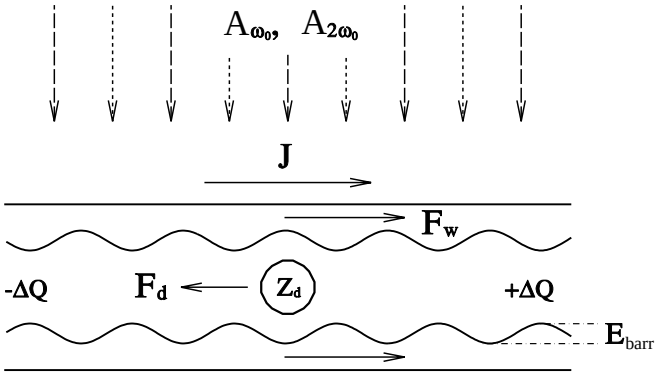

FIG. 1. Functional scheme of a nanotube-based atomic pump. Combined laser excitation at frequencies ω_0 and $2\omega_0$ induces a current J in the tube, which exerts the wind force F_w on an atom carrying the net charge Z_d. Reflected carriers build up a charge $\pm\Delta Q$, which generates a local field causing a direct force F_d to act on the atom. The atomic motion in the tube occurs on a potential energy surface with activation barriers E_{barr}.

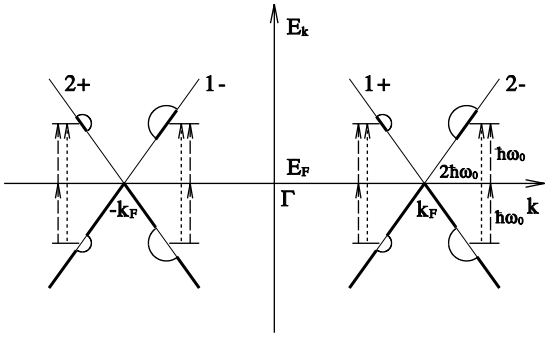

FIG. 2. Schematic of laser-induced one- and two-photon transitions at the respective energies $2\hbar\omega_0$ (long-dashed lines) and $\hbar\omega_0$ (dashed lines) between the crossing bands of a $(10, 10)$ carbon nanotube. Because of coherent mixing of these processes connecting the same states, the generation at the right-hand side of the crossing points $\pm k_F$ exceeds that on the left-hand side, resulting in a nonzero current along the tube.

with bands crossing at E_F (see Fig. 2), is

$$H = \sum_{\alpha=\pm1,\pm2;k} \pm\hbar k v_F c^+_{\alpha,k} c_{\alpha,k} + H_{\text{el-tw}} - \frac{e}{c} A(t) \sum_k (v_{1\mp2\pm}(k) c^+_{1\mp,k} c_{2\pm,k} + \text{H.c.}) + \sum_k [V^s_{\text{at}}(k,\bar{k},t) c^+_{1\mp,k} c_{2\pm,\bar{k}} + \text{H.c.}] + H_{\text{el-at}}(t). \quad (1)$$

The summation over the wave vector k extends near the two Fermi points $\pm k_F$ in the one-dimensional Brillouin zone of the tube. $\bar{k}$ is center symmetric to k with respect to the closest $\pm k_F$. The index $\alpha = \pm1, \pm2$ denotes the bands, with the sign indicating the direction of the intraband velocity. $H_{\text{el-tw}}$ describes the scattering of electrons by twistons [25] and other excitations. The third term describes interband transitions; $A(t) = A_{\omega_0} e^{-i(\omega_0 t+\theta_{\omega_0})} + A_{2\omega_0} e^{-i(2\omega_0 t+\theta_{2\omega_0})}$ + c.c. is the component along the tube axis of the vector potential for the laser fields, and $v_{1\mp2\pm}(k) = \langle k, 1\mp|(-i\hbar/m_e)\nabla_{\text{axis}}|k, 2\pm\rangle$ are interband velocity matrix elements. The last two terms in Eq. (1) describe the scattering of electrons by the atom and the dynamical charge transfer to the atom.

The lowest bands of the $(10, 10)$ tube near the Fermi points $\pm k_F$ are shown schematically in Fig. 2, with the populated regions for $E_k < E_F$ emphasized by thick lines. We show only the one- and two-photon transitions at the respective frequencies $2\omega_0$ and ω_0, connecting the same states; one-photon transitions at ω_0, not contributing to current, are neglected. Coherent mixing of the transition amplitudes for the one- and two-photon transitions can be controlled to yield different generation rates to the left and to the right of the Fermi points $\pm k_F$, symbolized by the different diameter of the half-circles, resulting in a nonzero current J.

In the rotating-wave approximation, the coherent sum of the one- and two-photon terms gives, for the effective generation field at k to the right of $\pm k_F$ [26],

$$\mathcal{A}_{\text{eff}}(k) = A_{2\omega_0} e^{-i\theta_{2\omega_0}} + \frac{\delta v(k)}{\hbar\omega_0} \frac{e}{c} (A_{\omega_0} e^{-i\theta_{\omega_0}})^2. \quad (2)$$

Only the crossing bands in Fig. 2 were included as *virtual* states in the two-photon part of Eq. (2) [26], where $\delta v(k) = 2v_F$ is the difference of the final (bands $1-$, $2-$) and initial (bands $2+$, $1+$) state velocities at k. The analogous expression for $\mathcal{A}_{\text{eff}}(\bar{k})$ at $\bar{k}$ to the left of $\pm k_F$ uses $\delta v(\bar{k}) = -2v_F$. Therefore, the amplitudes of $|\mathcal{A}_{\text{eff}}|$ at k and $\bar{k}$, and thus the generation rates there, can be different, and the resulting population imbalance of momenta near $\pm k_F$ creates a current. The direction and magnitude of this current are controlled by the phases θ_{ω_0}, $\theta_{2\omega_0}$ and the sign of the prefactor $\delta v(k)$, which is largely material independent. Consequently, the direction of the current that drives atoms in the pump can be controlled in single-wall and multiwall nanotubes or nanotube ropes.

The photogenerated current J, shown in Fig. 1, can be calculated from the Boltzmann equation in the relaxation time approximation [26,27]. In steady state it is given by

$$J = \frac{2e}{\hbar^2} \sigma_f^2 \tau_{\text{tr}}. \quad (3)$$

Here all bands in Fig. 2 and the two spin orientations are included, and τ_{tr} is the transport time in the tube. σ_f^2 is the product of the one- and two-photon terms in $(e/c)^2|\mathcal{A}_{\text{eff}}(k)|^2$ and of $|v_{2-1+}(k)|^2$, yielding

$$\sigma_f^2 = \frac{4e^3 v_F}{c^3\hbar\omega_0} |v_{2-1+}(k)|^2 A_{2\omega_0} (A_{\omega_0})^2 \cos(\delta\theta), \quad (4)$$

where the relative phase $\delta\theta = \theta_{2\omega_0} - 2\theta_{\omega_0}$ controls the direction of J. It is convenient to introduce the difference Δn in density of electrons traveling "right" and "left." Taking into account the contributions from all states near E_F, Δn is related to the current by $J = 4ev_F\Delta n$, which yields $\Delta n = \sigma_f^2 \tau_{\text{tr}}/(2\hbar^2 v_F)$.

To sustain atomic motion within the atomic pump, the force F due to the current J must be sufficiently large. Generation of such large forces F requires strong light intensities, excessively heating the tube. The absorbed power P depends in a linear way on the laser intensities I_{ω_0} and $I_{2\omega_0}$, whereas F is proportional to the product $I_{\omega_0} I_{2\omega_0}^{1/2}$. Therefore, the F/P ratio can be maximized using shorter laser pulses at higher intensities. The driving can also be increased by decreasing the frequency ω_0, since the factor $A_{2\omega_0}(A_{\omega_0})^2/\omega_0$ in Eq. (4) gives $\sigma_f^2 \propto \omega_0^{-4}$. In semiconducting nanotubes, one-photon absorption at ω_0 can be suppressed by tuning ω_0 in the gap, which changes the absorbed power dependence to $P \propto I_{\omega_0}^2$. Therefore, both I_{ω_0} and the ratio F/P can be sharply increased.

Our numerical estimates show that $I_{\omega_0} = I_{2\omega_0} = 100\ \text{kW/cm}^2$ at $\hbar\omega_0 = 100$ meV are reasonable values for these laser intensities. The interband velocity matrix elements are estimated to be $|v_{2-1+}(k)| \approx v_F \approx 1$ nm/fs [25,26], and the transport time due to scattering on

twistons is roughly $\tau_{\rm tr} \approx 300/T[{\rm K}]$ ps. This value is based on the resistance of several ropes [25], extrapolated to a single tube. Then, using Eq. (4), we obtain $\sigma_f^2 = 0.47\ ({\rm meV})^2$. At $T = 300$ K, Eq. (3) yields the current $J = 0.38\ \mu$A and the electron density difference $\Delta n = 0.6 \times 10^{-3}\ {\rm nm}^{-1}$ in the empty tube.

When intercalated in a nanotube, atoms often become partly ionized. The close similarity between fullerenes, nanotubes, and graphite also suggests that the interaction energies between atoms and these sp^2 bonded systems are similar [28]. Therefore we use the potential energy barriers $E_{\rm barr}$ and net charges Z_d of atoms encapsulated in C_{60} [29] also for nanotubes. In the following, we consider Lithium atoms with $Z_d = +0.6e$ and $E_{\rm barr} = 0.12$ eV. Calculations show that the tube band structure is not deformed much by the added atom. The chemical potential, however, shifts locally [15], thus attracting the delocalized transferred electrons and consequently screening the atom potential to a value $V_{\rm at}^s$ [30]. Further contribution to screening comes from the injected carriers that are also partly reflected by $V_{\rm at}^s$ [17]. In absence of experimental data, we assume $R \approx 0.1$ as a plausible value for the reflection coefficient of electrons on $V_{\rm at}^s$.

This electron reflection generates a net wind force on the intercalated atom. The momentum transferred within a unit length l_0 of the tube is $\delta p/l_0 = (2\hbar\delta k)(4\Delta n)R = (8\hbar\omega_0/v_F)(\Delta n)R$, where $\delta k = k - \bar{k}$. Based on the parameter values determined above, the momentum transferred per unit time yields $F_w = (\delta p/l_0)v_F = (4\omega_0/\hbar v_F)\sigma_f^2\tau_{\rm tr}R \approx 44\ \mu$eV/nm for the wind force and $F_w \propto T^{-1}$ for its temperature dependence. The effect of F_w on a partly ionized atom can be viewed as equivalent to a fictitious electric field, which in our case has a value $(e/Z_d)44$ V/mm.

Electrons reflected from the intercalated atom build up a local excess charge $\Delta Q_\pm \approx \pm 2e(\Delta n)l_{mfp}R$, separated about half of the mean-free path $l_{mfp} = v_F\tau_{\rm tr}$ from the atom. Neglecting screening, the resulting dipole creates locally an electric field $E = -16e(\Delta n)R/l_{mfp}$. The Li atom carrying a charge $Z_d = +0.6e$ experiences a direct force $F_d = Z_dE = 8Z_de\sigma_f^2R/(\hbar v_F)^2 \approx -0.8\ \mu$eV/nm. Since the ratio $F_w/F_d = \hbar\omega_0\tau_{\rm tr}v_F/2Z_de$ can be tuned to be very large ($\approx$58 here), our situation differs from the case of dc bias driving, where F_d dominates or is comparable to F_w both in bulk semiconductors [18] and metals [19].

The dynamics of the intercalated atom, as it diffuses along (across) the tube, is also influenced by the time dependence of $V_{\rm at}^s(t)$ and $H_{\text{el-at}}(t)$. In the transition state of hopping, the atom may block the electron transport more efficiently, thus modifying R and consequently the net force $F = F_w + F_d$, and form new electron tunneling channels for transport. As these effects are very difficult to estimate quantitatively, we neglect them and evaluate the average drift velocity of the added atom using steady-state forces.

In the presence of the current J, the barriers for intersite hopping $E_{\rm barr}$ are shifted by the product of the net force on the atom F and the vector of length $l_t = 1.42$ Å that connects neighboring sites. Consequently, hopping rates towards left and towards right are given by $\nu_{L,R} = \nu_0 \exp[-(E_{\rm barr} \pm Fl_t)/(k_BT)]$, where $\nu_0 = [(2E_{\rm barr})/(m_{\rm at}l_t^2)]^{1/2}$ is the atomic vibration frequency ($\nu_0 = 1.5 \times 10^{13}\ {\rm s}^{-1}$ for Li). This yields the drift velocity

$$\langle v_{\rm at}\rangle = (\nu_L - \nu_R)l_t \approx \frac{2\nu_0 F l_t^2}{k_BT}\exp\left(-\frac{E_{\rm barr}}{k_BT}\right). \quad (5)$$

The drift velocity $\langle v_{\rm at}\rangle$ of the Li atom, given by Eq. (5), is shown in Fig. 3 as a function of temperature. It grows fast at low temperatures, reaches a maximum at $T \approx 700$ K, and then decreases slowly. At $T = 300$ K, $\langle v_{\rm at}\rangle$ is more than 2 orders of magnitude smaller than the speed of broadening of the atom distribution by diffusion.

Exposure to the intense laser fields heats the nanotube, thus affecting the atomic transport. We estimate the average tube temperature T for laser pulses of duration t_p that repeat with a period of $t_{\rm rep} = 1$ s. Assuming that in graphite radiation penetrates the topmost 30 layers, then a surface area s_1 of the tube should absorb the power $P = (I_{\omega_0} + I_{2\omega_0})(s_1/15)(t_p/t_{\rm rep})$. Because of their mesoscopic nature, carbon nanotubes have limited emissivity in the long wavelength region. If approximated by a blackbody, power radiated out yields in steady state $P = \sigma T^4 s_1$, where $\sigma = 5.67 \times 10^{-8}\ {\rm W\,m^{-2}\,K^{-4}}$ is the Stefan-Boltzmann constant. For the above intensities, the dependence of the tube temperature $T = (2.35t_p[fs])^{1/4}$ K on the pulse length t_p is shown by the dashed line on the right-hand vertical scale of Fig. 3. The average atomic displacement during this laser pulse is $\langle x\rangle = \langle v_{\rm at}\rangle t_p$. Thus $t_p = 15$-μs-long pulses raise the tube temperature to $T \approx 430$ K and cause displacements of $\langle x\rangle = 0.3\ \mu$m, comparable to the tube length.

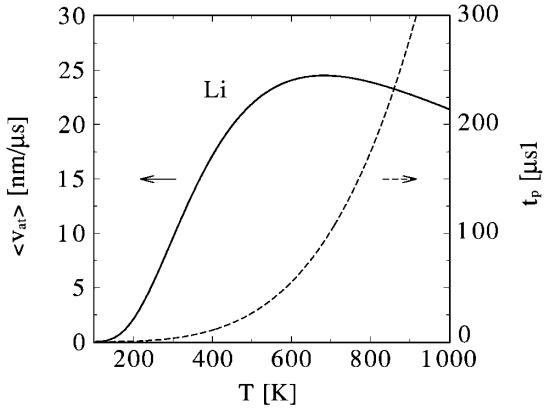

FIG. 3. The temperature dependence of the average drift velocity $\langle v_{\rm at}\rangle$ of a Li atom in a nanotube is given by the solid line. The relationship between the tube temperature T and the duration t_p of the laser pulse (right-hand vertical scale) is given by the dashed line.

Electrons excited by laser to the energy $\hbar\omega_0 = 100$ meV above E_F may also scatter inelastically from the intercalated atom and thus "heat" it above the tube temperature T [31]. Assuming that the atom thermally equilibrates after each hop, which occurs statistically every $t_b = \exp(E_{\text{barr}}/k_BT)/\nu_0 = 7$ ps at $T = 300$ K, it can absorb several phonons of the energy $h\nu_0 \approx 58$ meV $\approx E_{\text{barr}}/2$. Its "temperature," thus raised by tens to hundreds of degrees Kelvin above T, enters into the exponent of the activation factor in Eq. (5). This causes a significant increase of the velocity $\langle v_{\text{at}} \rangle$, in particular at low T or in the case of stronger driving, and it can also dramatically improve atom detachment from various tube imperfections.

Large defects, such as bamboo closures within multiwall tubes, obviously block atomic transport and must be eliminated by destroying the corresponding nanotube section. Charge accumulating at the tube ends also acts as a defect by generating an additional direct force $\tilde{F}_d$ that drags positively charged atoms in the same direction as F_w. This charge is continuously released by electrons or ions entering and leaving the tube. Consequently, tube ends and other small defects act as a rather soft trap potential $V(x)$, yielding a distribution $\rho_{\text{at}}(x) \propto \exp[-V(x)/k_BT]$ of aggregated atoms. Thermal fluctuations of trapped atoms at the aggregate boundaries can be largely augmented by the absorption of phonons from hot electrons. The combined effect of atom detaching/driving by two laser beams might also be achieved if one laser beam (hot electron detaching) and a dc bias (driving by F_d) are applied to the nanotube.

In summary, we have proposed a molecular pump with a (carbon) nanotube body. Excitation of the nanotube by two laser beams in a coherent control scheme generates an electron current, which drives intercalated atoms by the wind force F_w. The temperature dependence of the drift velocity v_{at} for a Li atom shows a pronounced maximum at $\langle v_{\text{at}} \rangle \approx 25$ nm/μs. The detachment rate and the drift velocity of the atom can be enhanced by inelastic scattering of hot electrons. The pump can be used for a semicontinuous deposition of atoms on surfaces. Two beam irradiation of surfaces may also be used to locally control diffusion at surfaces [32] and inside layered or porous materials [33].

P. K. thanks J. E. Sipe for support provided by Photonics Research, Ontario, and D. T. acknowledges financial support from the Office of Naval Research under Grant No. N00014-99-1-0252.

[1] D. M. Eigler and E. K. Schweizer, Nature (London) **344**, 524 (1990).
[2] J. A. Stroscio and D. M. Eigler, Science **254**, 1319 (1991).
[3] I.-W. Lyo and Ph. Avouris, Science **253**, 173 (1991).
[4] M. F. Crommie, C. P. Lutz, and D. M. Eigler, Science **262**, 218 (1993).
[5] M. Böhringer *et al.*, Phys. Rev. B **57**, 4081 (1998).
[6] K. Svoboda *et al.*, Nature (London) **365**, 721 (1994); L. P. Faucheux *et al.*, Phys. Rev. Lett. **74**, 1504 (1995); R. D. Astumian, Science **276**, 917 (1997).
[7] V. A. Lombillo, R. J. Stewart, and J. R. McIntosh, Nature (London) **373**, 161 (1995).
[8] S. Iijima, Nature (London) **354**, 56 (1991).
[9] A. Rubio *et al.*, mtrl-th/9508011; A. Rubio, J. L. Corkill, and M. L. Cohen, Phys. Rev. B **49**, 5081 (1994).
[10] J. W. Mintmire, B. I. Dunlap, and C. T. White, Phys. Rev. Lett. **68**, 631 (1992).
[11] N. Hamada, S. Sawada, and A. Oshiyama, Phys. Rev. Lett. **68**, 1579 (1992).
[12] R. Saito *et al.*, Appl. Phys. Lett. **60**, 2204 (1992).
[13] P. M. Ajayan *et al.*, Phys. Rev. Lett. **72**, 1722 (1994).
[14] G. Gao, T. Cagin, and W. A. Goddard III, Phys. Rev. Lett. **80**, 5556 (1998); L. Grigorian *et al.*, Phys. Rev. Lett. **80**, 5560 (1998).
[15] Y. Miyamoto *et al.*, Phys. Rev. Lett. **74**, 2993 (1995).
[16] T. J. Gramila *et al.*, Phys. Rev. Lett. **66**, 1216 (1991); A.-P. Jauho and H. Smith, Phys. Rev. B **47**, 4420 (1993).
[17] R. S. Sorbello, Phys. Rev. B **39**, 4984 (1989).
[18] D. Kandel and E. Kaxiras, Phys. Rev. Lett. **76**, 1114 (1996).
[19] A. Lodder and J. P. Dekker, in *Stress Induced Phenomena in Metalliation*, edited by H. Okabayashi and P. S. Ho, AIP Conf. Proc. No. 418, (AIP, New York, 1998), p. 315–328 (cond-mat/9803172).
[20] G. Kurizki, M. Shapiro, and P. Brumer, Phys. Rev. B **39**, 3435 (1989).
[21] E. Dupont *et al.*, Phys. Rev. Lett. **74**, 3596 (1995); R. Atanasov *et al.*, Phys. Rev. Lett. **76**, 1703 (1996).
[22] J. W. G. Wildöer *et al.*, Nature (London) **391**, 59 (1998).
[23] Y.-K. Kwon, S. Saito, and D. Tománek, Phys. Rev. B **58**, R13 314 (1998).
[24] A. Thess *et al.*, Science **273**, 483 (1996).
[25] C. L. Kane *et al.*, cond-mat/9704117.
[26] P. Král and J. Sipe, in Proceedings of the ICPS24 Conference, Jerusalem, 1998 (to be published).
[27] P. Král, Phys. Rev. B **53**, 11 034 (1996).
[28] Y.-K. Kwon *et al.*, Phys. Rev. Lett. **79**, 2065 (1997).
[29] Y. S. Li and D. TománekChem. Phys. Lett. **221**, 453 (1994); *ibid.* **243**, 42 (1995).
[30] M. F. Lin and D. S. Chuu, Phys. Rev. B **55**, 4996 (1997).
[31] K. S. Ralls, D. C. Ralph, and R. A. Buhrman, Phys. Rev. B **40**, 11 561 (1989).
[32] I. Derényi, Ch. Lee, and A.-L. Barabási, Phys. Rev. Lett. **80**, 1473 (1998).
[33] S. Furusawa, T. Suemoto, and M. Ishigame, Phys. Rev. B **38**, 12 600 (1988).